

A comparative study of the low energy HD+*o*-/*p*-H₂ rotational excitation/de-excitation collisions and elastic scattering

Renat A. Sultanov^{1,2,1,a)} Dennis Guster^{2,b)} and S. K. Adhikari^{1,c)}

¹⁾*Instituto de Física Teórica, UNESP – Universidade Estadual Paulista, 01140 São Paulo, SP, Brazil*

²⁾*Department of Information Systems & BCRL, St. Cloud State University, St. Cloud, MN, USA*

(Dated: 16 February 2019)

The precise Diep and Johnson H₂-H₂ potential energy surface (PES)¹, obtained from the first principles has been adjusted through appropriate rotation of the three-dimensional coordinate system and applied to low-temperature ($T < 300$ K) HD+*o*-/*p*-H₂ collisions of astrophysical interest. A non-reactive quantum mechanical close-coupling method is used to carry out computation for the total rotational state-to-state cross sections and thermal rate coefficients. A comparative study with previous calculations is presented.

PACS numbers: 34.50.-s, 34.20.-b, 34.20.Gj

I. INTRODUCTION

The simplest quantum-mechanical scattering problem, that between two hydrogen molecules, has been a formidable challenge to chemists and physicists working in this area. This is because the elastic and inelastic H₂+H₂ scattering have all the complications of a complex molecular scattering process like rotational and vibrational excitations and de-excitations. Many theoretical and experimental methods have been developed and used for the study of these processes^{1–15}. Additionally, there has been great interest in the study of HD+H₂ scattering. Although, this system bears some similarity with H₂+H₂, the identical system symmetry is broken here and hence many aspects of the theoretical formulation can be tested in the system under different symmetry conditions^{4,16–22}.

The PESs of H₂+H₂ and HD-H₂ are basically the same six-dimensional functions. The fact follows from a general theoretical point of view and the Born-Oppenheimer model²³. However, from an intuitive physical point of view, the two collisions should have rather different scattering output. This is because the H₂ and HD molecules have fairly different rotational constants and rotational-vibrational spectrum. They have different internal symmetries and dipole moments. Collisional properties of these systems are expected to be highly sensitive to dipole moments. Further, the HD-H₂ PES can be derived from H₂+H₂ by adjusting the coordinate of the center of mass of the HD molecule. Once the symmetry is broken in H₂+H₂ by replacing the H by the D atom in one H₂ molecule one can obtain the HD-H₂ PES. The new potential has all parts of the full HD-H₂ interaction including HD's dipole moment. However, in a case when a PES

is formulated for fixed interatomic coordinates between the two hydrogen atoms in the H₂-H₂ system, it would be difficult to extract the PES of HD-H₂, because the position of the HD center of mass is different from that of H₂. In this work we apply a rotational method for calculation of the HD-H₂ PES from that of H₂-H₂. The method is based on a rotation of the three-dimensional space from the body-fixed H₂-H₂ coordinate system to appropriately adjust the HD molecule center of mass.

The hydrogen molecule plays an important role in many areas of astrophysics. For example, the interstellar medium (ISM) cooling process is associated with the energy loss after inelastic collisions of the particles. These processes convert the kinetic energy of ISM's particles to their internal energies: for instance, in the case of molecules to their internal energy of rotational-vibrational degrees of freedom. Therefore, in order to accurately model the thermal balance and kinetics of ISM one needs accurate state-to-state cross sections and thermal rate constants. Theoretical state-resolved treatment requires precise PES of H₂-H₂, and a reliable dynamical method for H₂+H₂/HD collision^{5,16,21}. However, on the other hand, experimental measurements of these cross sections is a very difficult technical problem. Unfortunately, up to now no reliable experiments are available on these collision processes, which have important astrophysical applications. Moreover, different calculations with various H₂-H₂ PESs showed rather different results for important H₂+H₂ thermal rate coefficients.

The possible importance of the HD cooling in ISM was first noted in 1972 by Dalgarno and McCray²⁴. Because of the special properties of HD this molecule is even more effective cooler than H₂. This happens at low temperatures $T < 100$ K²⁴, where the cooling function of HD becomes ~ 15 times larger than the H₂ cooling function²⁴. As we mentioned in the previous paragraph, to carry out calculation of the cooling function one needs to know precise cross sections and thermal rate coefficients of the rotational-vibrational energy transfer collisions. That is why there is a constant interest to reliable

^{a)}Electronic mail: rasultanov@stcloudstate.edu

^{b)}Electronic mail: dcguster@stcloudstate.edu

^{c)}Electronic mail: adhikari@ift.unesp.br;
http://www.ift.unesp.br/users/adhikari

quantum-mechanical computation of different rotational-vibrational atom-molecular energy transfer collision cross sections and corresponding thermal rate coefficients^{25–29}.

A realistic full-dimensional *ab initio* PES for the H₂-H₂ system was first constructed by Schwenke³⁰ and that potential was widely used in a variety of methods and computation techniques. Flower²¹ used Schwenke's H₂-H₂ PES³⁰ in a study of H₂-HD collision. Later on, new extensive studies of the H₂-H₂ system by Diep and Johnson (DJ)¹ and Boothroyd *et al.* (BMKP)³¹ have produced refined PES for the H₂-H₂ system. These PESs have been used in several different calculations^{32–36}. However, in our previous works^{12,34} we found that in the case of low energy H₂+H₂ collision these PESs provide different results for some specific state-resolved cross sections. The difference may be up to an order of magnitude. This fact was also confirmed in work¹³. The BMKP PES, probably, needs future improvements^{12,13,34}, because the DJ PES gives better agreement with existing experiments for H₂+H₂ than the BMKP potential.

Nonetheless, as a first trial Sultanov *et al.* applied the BMKP PES to the low-energy HD+H₂ collisions after appropriate modification^{37,38}. When the results of these calculations^{37,38} were compared with prior studies^{5,21} a relatively good agreement was found with Schaefer's results⁵. At the same time substantial differences with the newer data obtained by Flower was noted²¹. Therefore, in the light of these circumstances, it would be useful to apply another modern H₂-H₂ PES¹ to HD-H₂ collisions. The DJ potential was formulated specifically for the symmetric H₂-H₂ system when distances between hydrogen atoms are fixed at a specific equilibrium value in each H₂ molecule. In this paper we provide the first calculation describing collisions of rotationally excited H₂ and HD molecules using the DJ PES. We also provide a comparison with our previous calculations^{37,38} with the BMKP PES, which is a global six-dimensional surface.

In Sec. II we briefly outline the quantum-mechanical close-coupling approach and our method to convert the symmetric DJ PES to be appropriate for calculations of the HD+H₂ system. We represent results for selected state-to-state cross sections and thermal rate coefficients for rotational excitation/de-excitation of HD in low-energy collisions with *o*-p-H₂ in Sec. III. Finally, in Sec. IV we present a brief summary of our findings and conclusion.

II. COMPUTATIONAL METHOD

A. Dynamical equations

The Schrödinger equation for the (12)+(34) collision in the center-of-mass frame, where 1, 2, 3 and 4 are atoms and (12) and (34) are diatomic molecules modeled by

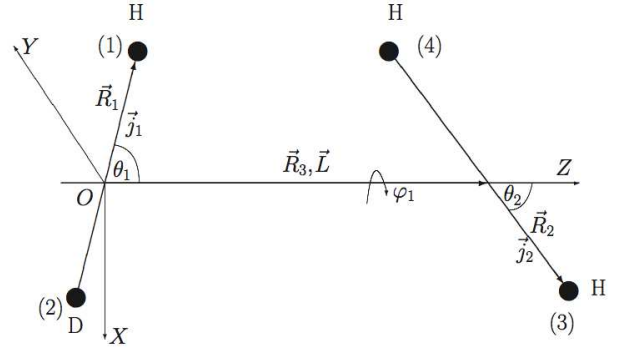


FIG. 1. (Color online) Four-atomic system (12) + (34) or HD+H₂, where H is a hydrogen atom and D is deuterium, represented by few-body Jacobi coordinates: \vec{R}_1 , \vec{R}_2 , and \vec{R}_3 . The vector \vec{R}_3 connects the center of masses of the HD and H₂ molecules and is directed over the axis OZ, θ_1 is the angle between \vec{R}_1 and \vec{R}_3 , θ_2 is the angle between \vec{R}_2 and \vec{R}_3 , φ_1 is the torsional angle, j_1 , j_2 , L are quantum angular momenta over the corresponding Jacobi coordinates \vec{R}_1 , \vec{R}_2 , and \vec{R}_3 .

linear rigid rotors, is^{3,39,40}

$$\left[\frac{P_{\vec{R}_3}^2}{2M_{12}} + \frac{L_{\vec{R}_1}^2}{2\mu_1 R_1^2} + \frac{L_{\vec{R}_2}^2}{2\mu_2 R_2^2} + V(\vec{R}_1, \vec{R}_2, \vec{R}_3) - E \right] \Psi(\hat{R}_1, \hat{R}_2, \vec{R}_3) = 0, \quad (1)$$

where $P_{\vec{R}_3}$ is the momentum operator of the kinetic energy of collision, \vec{R}_3 is the collision coordinate, whereas \vec{R}_1 and \vec{R}_2 are relative vectors between atoms in the two diatomic molecules as shown in the Fig. 1, and $L_{\hat{R}_{1(2)}}$ are the quantum-mechanical rotation operators of the rigid rotors. Here, $M_{12} \equiv [(m_1 + m_2)(m_3 + m_4)]/[(m_1 + m_2 + m_3 + m_4)]$ is the reduced mass of the two diatomic molecules (12) and (34) and $\mu_{1(2)} \equiv [m_{1(3)}m_{2(4)}]/[(m_{1(3)} + m_{2(4)})]$ are reduced masses of the two molecules. The vectors $\hat{R}_{1(2)}$ are the angles of orientation of rotors (12) and (34), respectively; $V(\vec{R}_1, \vec{R}_2, \vec{R}_3)$ is the PES for the four-atomic system (1234), and E is the total energy in the center-of-mass system. The linear rigid-rotor model used in this calculation was already applied in some previous studies^{21,39,40}. For the considered range of kinetic energies of astrophysical interest the model is quite justified.

The eigenfunctions of the operators $L_{\hat{R}_{1(2)}}$ in Eq. (1) are simple spherical harmonics $Y_{j_i m_i}(\hat{r})$. To solve this equation the following angular-momentum expansion is used:

$$\Psi(\hat{R}_1, \hat{R}_2, \vec{R}_3) = \sum_{JM j_1 j_2 j_{12} L} \frac{U_{j_1 j_2 j_{12} L}^{JM}(R_3)}{R_3} \times \phi_{j_1 j_2 j_{12} L}^{JM}(\hat{R}_1, \hat{R}_2, \vec{R}_3) \quad (2)$$

where $U_{j_1 j_2 j_{12} L}^{JM}(R_3)$ are unknown coordinate functions, J is total angular momentum quantum number of the

(1234) system and M is its projection onto the space fixed Z axis, and channel expansion functions are the following:

$$\begin{aligned} \phi_{j_1 j_2 j_{12} L}^{JM}(\hat{R}_1, \hat{R}_2, \vec{R}_3) = \sum_{\tilde{m}_1 \tilde{m}_2 \tilde{m}_{12} \tilde{m}} C_{j_1 \tilde{m}_1 j_2 \tilde{m}_2}^{j_{12} \tilde{m}_{12}} C_{j_{12} \tilde{m}_{12} L \tilde{m}}^{JM} \\ \times Y_{j_1 \tilde{m}_1}(\hat{R}_1) Y_{j_2 \tilde{m}_2}(\hat{R}_2) Y_{L \tilde{m}}(\vec{R}_3), \end{aligned} \quad (3)$$

here $j_1 + j_2 = j_{12}$, $j_{12} + L = J$, \tilde{m}_1 , \tilde{m}_2 , \tilde{m}_{12} and \tilde{m} are projections of j_1 , j_2 , j_{12} and L , respectively. The C 's are the appropriate Clebsch-Gordan coefficients. The quantum-mechanical momenta j_1 , j_2 and L over corresponding Jacobi vectors \vec{R}_1 , \vec{R}_2 and \vec{R}_3 are also shown in Fig. 1.

Upon substitution of Eq. (2) into Eq. (1), one obtains a set of coupled second order differential equations for the unknown radial functions $U_\alpha^{JM}(R_3)^{39,40}$

$$\begin{aligned} \left(\frac{d^2}{dR_3^2} - \frac{L(L+1)}{R_3^2} + k_\alpha^2 \right) U_\alpha^{JM}(R_3) \\ = 2M_{12} \sum_{\alpha'} \int \langle \phi_{\alpha'}^{JM}(\hat{R}_1, \hat{R}_2, \vec{R}_3) | V(\vec{R}_1, \vec{R}_2, \vec{R}_3) | \\ \phi_{\alpha'}^{JM}(\hat{R}_1, \hat{R}_2, \vec{R}_3) \rangle U_{\alpha'}^{JM}(R_3) d\hat{R}_1 d\hat{R}_2 d\hat{R}_3, \end{aligned} \quad (4)$$

where $\alpha \equiv (j_1 j_2 j_{12} L)$. We apply the hybrid modified log-derivative-Airy propagator in the general-purpose scattering program MOLSCAT⁴¹ to solve the coupled radial Eq. (4).

The log-derivative matrix is propagated to large inter-molecular distances R_3 , since all experimentally observable quantum information about the collision is contained in the asymptotic behavior of functions $U_\alpha^{JM}(R_3 \rightarrow \infty)$. The numerical results are matched to the known asymptotic solution to derive the scattering S -matrix $S_{\alpha\alpha'}^J$:

$$\begin{aligned} U_\alpha^J \sim_{R_3 \rightarrow +\infty} \delta_{\alpha\alpha'} e^{-i(k_{\alpha\alpha'} R_3 - l\pi/2)} - \sqrt{\frac{k_{\alpha\alpha'}}{k_{\alpha\alpha'}}} S_{\alpha\alpha'}^J \\ \times e^{-i(k_{\alpha\alpha'} R_3 - l'\pi/2)}, \end{aligned} \quad (5)$$

where $k_{\alpha\alpha'} = \sqrt{2M_{12}(E + E_\alpha - E_{\alpha'})}$ is the channel wave number, $E_{\alpha(\alpha')}$ are rotational channel energies for α and α' . The method was used for each partial wave until a converged cross section was obtained. It was verified that the results are converged with respect to the number of partial waves as well as the matching radius, R_{3max} , for all channels included in our calculation. The cross sections for rotational excitation and relaxation can be obtained directly from the S -matrix. In particular the cross sections for excitation from $j_1 j_2 \rightarrow j'_1 j'_2$ summed over the final $\tilde{m}'_1 \tilde{m}'_2$ and averaged over the initial $\tilde{m}_1 \tilde{m}_2$ are given by

$$\begin{aligned} \sigma(j'_1, j'_2; j_1 j_2, \epsilon) = \pi \sum_{J j_{12} j'_{12} L L'} (2J+1) \\ \times \frac{|\delta_{\alpha\alpha'} - S^J(j'_1, j'_2, j'_{12} L'; j_1, j_2, j_{12}, L; E)|^2}{(2j_1+1)(2j_2+1)k_{\alpha\alpha'}} \end{aligned} \quad (6)$$

The relative kinetic energy of the two molecules in the center of mass frame is:

$$\epsilon = E - B_1 j_1(j_1 + 1) - B_2 j_2(j_2 + 1), \quad (7)$$

where $B_{1(2)}$ are the rotation constants of rigid rotors (12) and (34), respectively, of total angular momentum $j_{1(2)}$. The relationship between the rotational thermal-rate coefficient $k_{j_1 j_2 \rightarrow j'_1 j'_2}(T)$ at temperature T and the corresponding cross section $\sigma_{j_1 j_2 \rightarrow j'_1 j'_2}(\epsilon)$, can be obtained through the following weighted average

$$\begin{aligned} k_{j_1 j_2 \rightarrow j'_1 j'_2}(T) = \frac{1}{(k_B T)^2} \sqrt{\frac{8k_B T}{\pi M_{12}}} \int_{\epsilon_s}^{\infty} \sigma_{j_1 j_2 \rightarrow j'_1 j'_2}(\epsilon) \\ \times e^{-\epsilon/k_B T} d\epsilon, \end{aligned} \quad (8)$$

where k_B is Boltzman constant and ϵ_s is the minimum relative kinetic energy of the two molecules for the levels j_1 and j_2 to become accessible.

B. The BMKP H₂-H₂ PES

The BMKP PES³¹, is a global six-dimensional potential energy surface for two hydrogen molecules. It was especially constructed to represent the whole interaction region of the chemical reaction dynamics of the four-atomic system and to provide an accurate van der Waals well. In the six-dimensional conformation space of the four-atomic system the PES forms a complicated three-dimensional hyper surface³¹. To compute the distances between the four atoms R_1, R_2 and R_3 , the BMKP PES uses Cartesian coordinates. Therefore it was necessary to convert spherical coordinates used in the close-coupling method⁴¹ to the corresponding Cartesian coordinates and compute the distances between the four atoms followed by calculation of the PES^{37,38}. Without the loss of generality the procedure used a specifically oriented coordinate system $OXYZ$ ³⁷. First we introduce the Jacobi coordinates $\{\vec{R}_1, \vec{R}_2, \vec{R}_3\}$ and the radius-vectors of all four atoms in the space-fixed coordinate system $OXYZ$: $\{\vec{r}_1, \vec{r}_2, \vec{r}_3, \vec{r}_4\}$ (not shown in Fig. 1). As in Ref.³⁷ we apply the following procedure: the center of mass of the HD molecule is put at the origin of the coordinate system $OXYZ$, and the \vec{R}_3 is directed to center of mass of the H₂ molecule along the OZ axis, as shown in Fig. 1. Then $\vec{R}_3 = \{R_3, \Theta_3 = 0, \Phi_3 = 0\}$, with Θ_3 and Φ_3 the polar and azimuthal angles, $\vec{R}_1 = \vec{r}_1 - \vec{r}_2$, $\vec{R}_2 = \vec{r}_4 - \vec{r}_3$, $\vec{r}_1 = \xi \vec{R}_1$ and $\vec{r}_2 = (1 - \xi) \vec{R}_1$, where $\xi = m_2/(m_1 + m_2)$.

Next, without the loss of generality, we can adopt the $OXYZ$ system in such a way, that the HD inter-atomic vector \vec{R}_1 lies on the XOZ plane. Then the angle variables of \vec{R}_1 and \vec{R}_2 are: $\hat{R}_1 = \{\Theta_1, \Phi_1 = \pi\}$ and $\hat{R}_2 = \{\Theta_2, \Phi_2\}$ respectively. One can see, that the Carte-

This transformation converts the initial Jacobi vectors in $OXYZ$: $\vec{R}_1 = \{R_1, \theta_1, \phi_{12}\}$, $\vec{R}_2 = \{R_2, \theta_2, 0\}$ and $\vec{R}_3 = \{R_3, 0, 0\}$ to the corresponding Jacobi vectors with new coordinates in the new $O'X'Y'Z'$: $\vec{R}'_1 = \{R'_1, \theta'_1, \phi'_{12}\}$, $\vec{R}'_2 = \{R'_2, \theta'_2, 0\}$ and $\vec{R}'_3 = \{R'_3, 0, 0\}$. As a result of this simple procedure we obtain a new PES, namely:

$$V_{DJ}^{H_2}(R_3, \theta_1, \theta_2, \phi_{12}) \rightarrow \tilde{V}_{DJ}^{HD}(R'_3, \theta'_1, \theta'_2, \phi'_{12}). \quad (20)$$

It is quite obvious, that the rotation does not affect the coordinate function $V_{1,l_2,l}(R_3)$ in Eq. (15). Note, in a previous calculation of low energy collision between monodeuterated ammonia NH_2D and a helium atom, a somewhat similar spatial rotational-translational procedure has been applied to the original PES of the NH_3 -He system⁴³.

Next, any rotation of the 3D $OXYZ$ coordinate system can be represented by Euler angles, i.e. $\{\alpha, \beta, \gamma\}$ ^{44,45}. In this work we choose the following Euler angles: $\{\alpha = 0, \beta = \eta, \gamma = 0\}$. To calculate the value of the rotational angle η in Fig. 2, one can consider the internal triangle $\triangle O_{HD}OO_{H_2}$ which is shown in Fig. 2. The angle η is determined from the following formula:

$$\cot \eta = \frac{(R'_3 + x \sin \theta'_2)}{x \cos \theta'_2}. \quad (21)$$

The derivation of (21) can be expressed as follows. First, the angles of the triangle $\triangle O_{HD}OO_{H_2}O$ satisfy the following equation $(\pi - \theta_2) + \eta + \theta'_2 = \pi$ or $\theta_2 = \eta + \theta'_2$. Secondly, based on the law of sines for $\triangle O_{HD}OO_{H_2}$:

$$\frac{x}{\sin \eta} = \frac{R}{\sin \theta'_2} = \frac{R'}{\sin \varepsilon}, \quad (22)$$

where $\varepsilon = \pi - \theta_2$. Because $\sin \varepsilon = \cos \theta_2$ we have:

$$\frac{x}{\sin \eta} = \frac{R}{\sin \theta'_2} = \frac{R'}{\cos \theta_2}, \quad (23)$$

and finally:

$$\frac{\cos(\eta + \theta'_2)}{\sin \eta} = \frac{R'}{x}, \quad (24)$$

from which one can directly obtain the expression (21). In such a way the rotation of the coordinate system from $OXYZ$ to $O'X'Y'Z'$ makes a corresponding transformation of the coordinates of the atoms in the 4-body system and the distance between two molecules. One has the following relations among old and new variables⁴⁴:

$$\cos(\theta_1) = \cos(\theta'_1) \cos(\eta) - \sin(\theta'_1) \sin(\eta) \cos(\phi'_{12}), \quad (25)$$

$$\cos(\theta_2) = \cos(\theta'_2) \cos(\eta) - \sin(\theta'_2) \sin(\eta) \cos(\phi'_{12}), \quad (26)$$

$$\cot(\phi_{12}) = \cot(\phi'_1) \cos(\eta) + \cot(\theta'_1) \frac{\sin(\eta)}{\sin(\phi'_{12})}, \quad (27)$$

$$R_3 = \sqrt{x^2 + R_3'^2 - 2xR_3' \cos(\theta'_2)}. \quad (28)$$

In the calculation of $HD+H_2$ with the DJ PES one has to use new coordinates $\theta'_1, \theta'_2, \phi'_{12}, R'_3$. However, the potential (15) has been expressed through the old H_2 - H_2 variables, hence it is to be transformed to new variables using Eqs. (25) – (28).

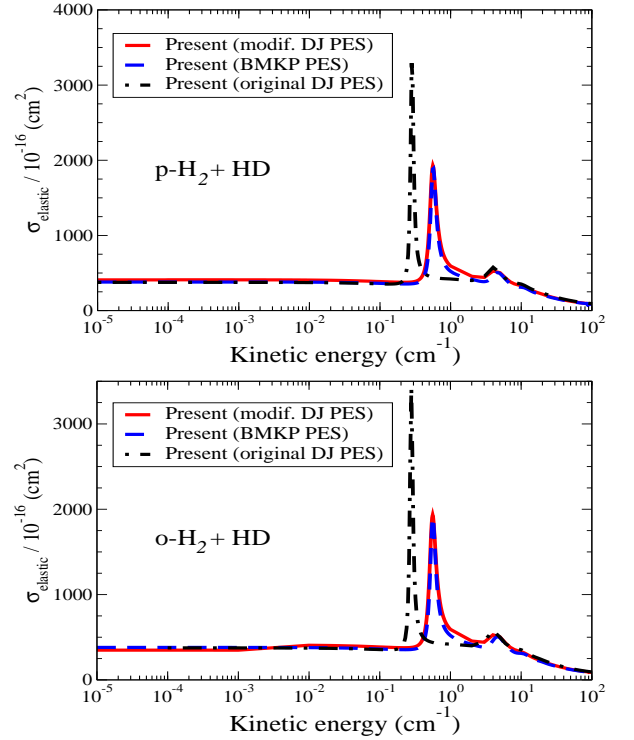


FIG. 3. (Color online) Elastic scattering total cross sections for $HD+o\text{-}H_2$ (upper panel) and $HD+p\text{-}H_2$ (lower panel) at different kinetic energies ϵ with the BMKP³¹ potential of Sec. IIB, the modified DJ¹ PES of Sec. IIC and the original DJ PES.

III. NUMERICAL RESULTS

Results for the low energy $HD+o/p\text{-}H_2$ elastic scattering cross-sections and few selected quantum-mechanical rotational transitions together with the corresponding results from previous studies^{37,38} are presented below. The cross sections are also compared with the corresponding results from⁵. Additionally, we compare our results for the thermal rate coefficients (8) with previous calculations^{5,21}. The results for the low energy elastic scattering cross sections cannot be compared with other theoretical/experimental data. To the best of our knowledge such calculations do not exist.

A. Elastic scattering

In Fig. 3 we show the present elastic scattering cross sections for $HD+o/p\text{-}H_2$ collisions at low and ultra-low energies calculated using three different potentials: the BMKP potential of Sec. IIB, the modified DJ potential of Sec. IIC, and the original DJ potential appropriate for the H_2 - H_2 system. In each cross section there is a prominent resonance. In Fig. 3 although the shapes of three cross sections are similar to each other the reso-

TABLE I. The elastic scattering cross sections σ_{el} (10^{-16}cm^2) at selected relative kinetic energies ϵ (cm^{-1}) and corresponding scattering lengths a_{scatt} (10^{-8}cm) in the $o\text{-}p\text{-H}_2 + \text{HD} \rightarrow o\text{-}p\text{-H}_2 + \text{HD}$ low energy collisions calculated with three different potentials: modified DJ PES from Sec. IIC and original BMKP³¹ and DJ¹ PESs. Numbers in parentheses are powers of 10.

ϵ (cm^{-1})	Elastic cross section: $\sigma_{el} \times 10^{-16}$ (cm^2)					
	$o\text{-H}_2 + \text{HD}$			$p\text{-H}_2 + \text{HD}$		
	mod. DJ	BMKP	DJ	mod. DJ	BMKP	DJ
4.0(-5)	348.61	380.70	375.29	408.68	380.02	375.87
5.0(-5)	348.61	380.70	375.29	408.68	380.02	375.87
1.0(-4)	348.59	380.67	375.27	409.96	380.00	375.86
1.0(-2)	406.4	378.1	372.5	406.6	378.5	373.0
1.0(-1)	386.4	362.2	355.3	386.6	362.5	355.8
3.0(-1)	385.0	359.0	1705.0	385.0	359.1	2039.8
4.0(-1)	467.3	418.9	516.26	466.1	416.9	529.0
6.0(-1)	1641.2	1577.6	433.8	1653.2	1611.5	437.0
1.0	592.0	520.1	419.3	593.3	522.6	421.0
5.0	504.4	492.9	501.5	504.4	492.8	501.8
10	331.1	310.7	353.3	331.1	310.6	353.1
100	87.6	84.6	93.2	87.6	84.6	93.1
Scattering length: $a_{scatt} \times 10^{-8}$ (cm)						
$\epsilon \rightarrow 0.0$	5.27	5.50	5.46	5.70	5.50	5.47

nance peak and the position of the resonance differ significantly when we use the original DJ potential without the modifications described in the Sec. II. This is because the original, symmetrical DJ potential¹ does not have all the asymmetrical features of the HD+H₂ interaction. Moreover, these features are of crucial importance for HD+H₂ scattering. In Table III we show the elastic cross sections $\sigma_{el}(\epsilon)$ for a few selected energies calculated with the three potentials. We also include in Table III the results for scattering lengths a_0 's. As can be seen from Fig. 3 and Table III we have obtained extremely good agreement between our calculations with the BMKP and with the modified DJ PESs. For the considered range of the kinetic energies we obtained full numerical convergence, for instance, the total angular momentum J was used up to the maximum value $J_{max} = 12$ in this calculation.

B. Non-elastic channels

The main goal of the present study is not to obtain results for every possible transition cross section in the HD+H₂ collision, but rather to demonstrate how the appropriately undertaken 3D rotation of the symmetrical surface of the H₂ - H₂ system could be adapted for collision of the H₂ and HD molecules. We carry out calculations for a fairly wide region of the collision energies, i.e. from 3 K to up to 300 K. This temperature interval is relevant for future calculations of the important HD-cooling function²⁴. Here we compute few transition cross sections in which we noticed substantial differences between our results obtained with the two different PESs from Refs.^{1,31} and also between our results and the data from previous studies^{5,21}.

In Figs. 4 to 8 we show these results for a few selected state-to-state HD+ $o\text{-}p\text{-H}_2$ integral cross sections. The results have been calculated with two different potentials, specifically, with the BMKP PES³¹ of Sec. IIB and the modified DJ PES of Sec. IIC. When possible we compare our results with existing previous calculations for the state-selected total cross sections and thermal rate coefficients. It is necessary to mention that the original DJ surface¹ cannot be correctly used for the non-elastic or transition channel calculations, i.e. for the rotational state transitions in an HD+H₂ collision. If the original, unmodified DJ potential is applied one can get extremely low numbers ($\sim 10^{-35}$) for the HD+H₂ rotational state-to-state probabilities and cross sections. That is why it was necessary to undertake the geometrical modifications to the DJ surface described in Sec. IIC. We obtained a fairly good agreement between our calculations with the use of the two PESs. Besides some qualitative differences in the state-resolved total cross sections the overall behavior of the cross section $\sigma_{j_1 j_2 \rightarrow j'_1 j'_2}(v)$ was found identical, where v is the relative velocity of the two molecules. However we obtained substantial differences between our $\sigma_{j_1 j_2 \rightarrow j'_1 j'_2}(v)$ cross sections and corresponding data from Ref.⁵.

In Fig. 4 we plot the total cross sections for the rotational transitions (02) - (20) and (13) - (11). The notation of the rotational quantum numbers can be understood by comparison to the following equations:

$$\text{HD}(0) + \text{H}_2(2) \rightarrow \text{HD}(2) + \text{H}_2(0), \quad (29)$$

$$\text{HD}(1) + \text{H}_2(3) \rightarrow \text{HD}(1) + \text{H}_2(1), \quad (30)$$

where the numbers in parenthesis denote rotational quantum numbers j_1, j_2 etc.. On the upper plot it is seen that while the two results of this study are in fairly good

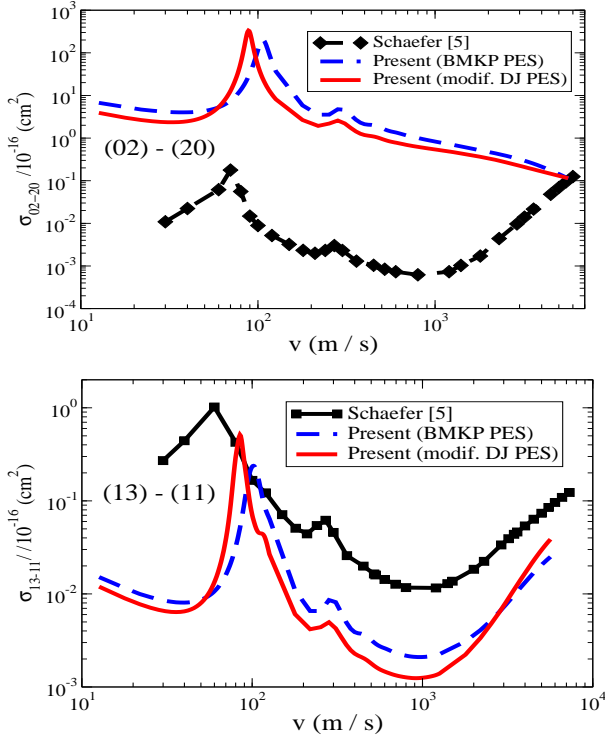


FIG. 4. (Color online) Total cross sections for transition $(02) \rightarrow (20)$ and $(13) \rightarrow (11)$, i.e. $\text{HD}(0)+\text{H}_2(2) \rightarrow \text{HD}(2)+\text{H}_2(0)$ (upper panel) and $\text{HD}(1)+\text{H}_2(3) \rightarrow \text{HD}(1)+\text{H}_2(1)$ (lower panel) for different velocities v . Present calculations with the BMKP⁵ and modified DJ PESs are compared with those of Ref.³¹.

agreement between each other we obtain substantial disagreements with the result of Ref.⁵. The same is true in the lower plot, although the behavior of these cross sections has a common character.

In Fig. 5 we show the cross sections for rotational transitions in $\text{HD}+\text{H}_2$ for the BMKP and the modified DJ PESs for the processes $\text{HD}(1)+\text{H}_2(3) \rightarrow \text{HD}(0)+\text{H}_2(1)$, and $\text{HD}(1)+\text{H}_2(3) \rightarrow \text{HD}(2)+\text{H}_2(1)$. The corresponding results from Ref.⁵ are also shown. We again obtain a fairly good agreement between our results computed with the BMKP and the modified DJ PESs, however, differing significantly from the corresponding Schaefer result⁵. Unfortunately we cannot compare these cross sections with the results of the calculation by Flower²¹, in which a different $\text{H}_2\text{-H}_2$ potential from³⁰ was used. This is because Flower's data includes results mostly for the thermal rate coefficients. However, within the next subsection in Table II we compare our few selected rotational state-resolved thermal rate coefficients with the corresponding results from Refs.^{5,21}.

From the astrophysical point of view, perhaps, one needs only precise rotational and in some rare cases vibrational state-to-state thermal rate coefficients $k_{j_1 j_2 \rightarrow j'_1 j'_2}(T)$ in H_2+H_2 , $\text{HD}+\text{H}_2$ etc. These quantities are less sensitive to interaction potentials. However, the

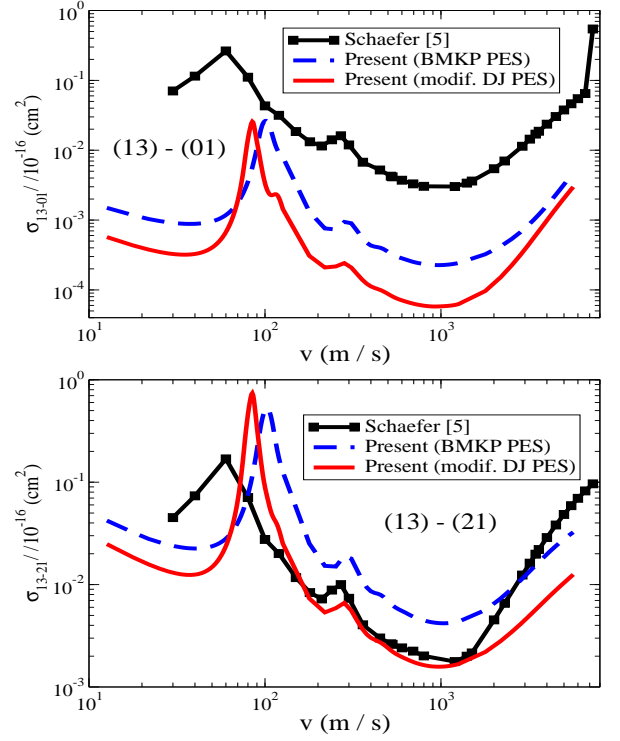


FIG. 5. (Color online) Same as Fig. 4 for transitions $(13) \rightarrow (01)$ and $(13) \rightarrow (21)$.

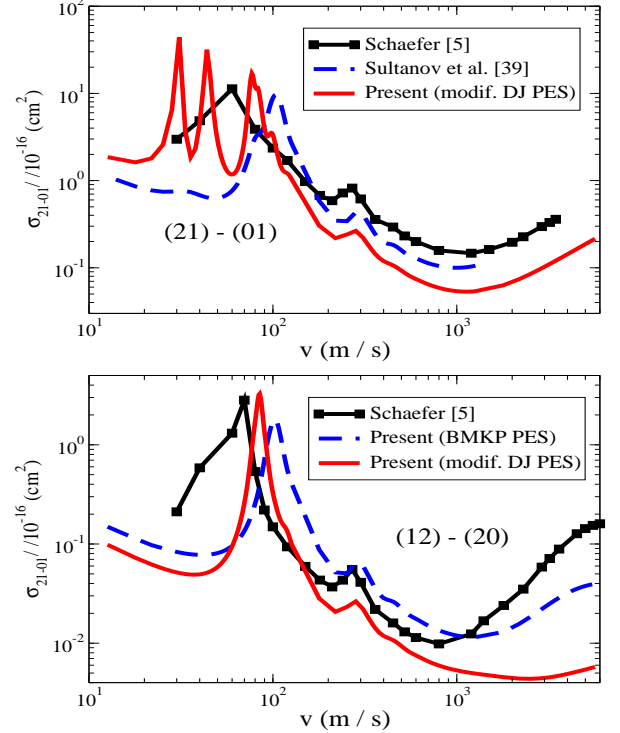


FIG. 6. (Color online) Same as Fig. 4 for transitions $(21) \rightarrow (01)$ and $(12) \rightarrow (20)$.

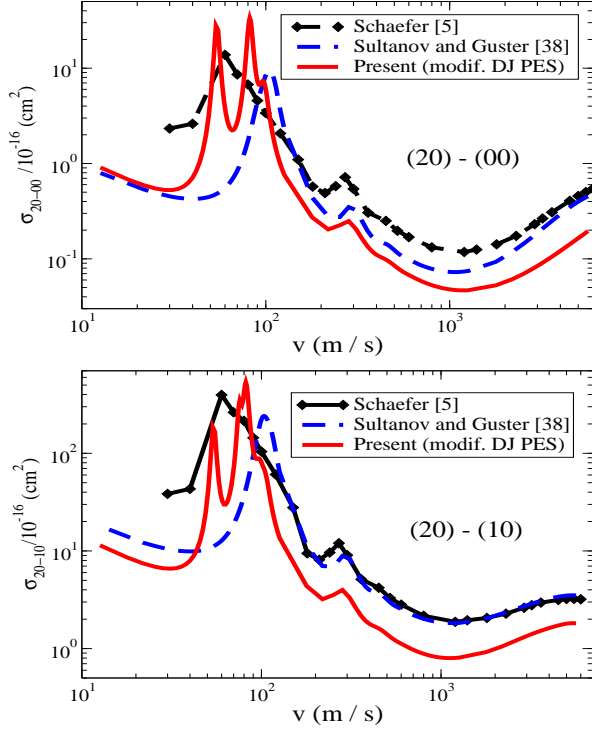


FIG. 7. (Color online) Same as Fig. 4 for transitions $(20) \rightarrow (00)$ and $(20) \rightarrow (10)$.

overall behavior of all possible state-selected cross sections should be very important for calculation of the thermal rates as seen in Fig. 4. It appears that the cross sections are much more sensitive to the PESs used in the calculations. Hence it is useful and even probably important in some specific cases to compare the cross sections from various calculations where different PESs have been used.

Further, Figs. 6 and 7 exhibit our results for the state-to-state rotational cross sections in transitions $\text{HD}(2) + \text{H}_2(1) \rightarrow \text{HD}(0) + \text{H}_2(1)$ and $\text{HD}(1) + \text{H}_2(2) \rightarrow \text{HD}(2) + \text{H}_2(0)$ and in transitions $\text{HD}(2) + \text{H}_2(0) \rightarrow \text{HD}(0) + \text{H}_2(0)$ and $\text{HD}(2) + \text{H}_2(0) \rightarrow \text{HD}(1) + \text{H}_2(0)$, respectively. We obtained fairly good agreement between our own results. Additionally, in these rotational transitions fairly good agreement with the corresponding cross sections from Ref.⁵ has also been obtained. Finally, Fig. 8 shows our integral cross section for the transition $\text{HD}(0) + \text{H}_2(2) \rightarrow \text{HD}(2) + \text{H}_2(0)$. This process is also interesting, because the transition occurs in the two molecules simultaneously. We would like to name such processes as double-transition processes.

C. Thermal rate coefficients

In Table II our rotational thermal rate coefficients $k_{j_1 j_2 \rightarrow j'_1 j'_2}(T)$ are presented. In this paper we choose only

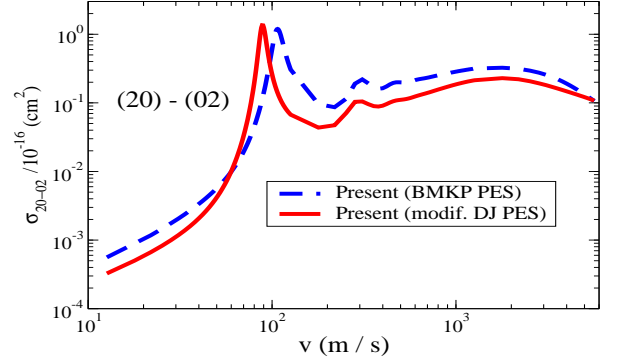


FIG. 8. (Color online) Same as Fig. 4 for transition $(20) - (02)$.

three rotational double-transitions in the collision: $(02) - (20)$, $(12) - (20)$, and $(20) - (02)$. These results were obtained from corresponding state-resolved integral cross sections $\sigma_{j_1 j_2 \rightarrow j'_1 j'_2}(\epsilon)$ with the use of the expression (8). In a previous study²¹, Flower compared his rotational transition thermal rate coefficients with the corresponding Schaefer data⁵ and found substantial differences between his results and results from Ref.⁵ even at high temperatures. The point is that in these processes the transition occurs in the two molecules simultaneously. In such rotational transitions the probabilities and cross sections should be very sensitive to the interaction potential. Perhaps, because of this reason the results of Refs.⁵ and²¹ differ so dramatically for transitions like $(02) - (20)$. In fact, we also obtained substantial differences between our thermal rates and with corresponding results from Refs.^{5,21}. Particularly the large differences were detected at the lower temperature regime.

In Table II we show our thermal rate coefficients $k_{j_1 j_2 \rightarrow j'_1 j'_2}(T)$ for the processes $\text{HD}(0) + \text{H}_2(2) \rightarrow \text{HD}(2) + \text{H}_2(0)$, and $\text{HD}(1) + \text{H}_2(2) \rightarrow \text{HD}(2) + \text{H}_2(0)$, and those for $\text{HD}(2) + \text{H}_2(0) \rightarrow \text{HD}(0) + \text{H}_2(2)$. We present our results calculated with the BMKP³¹ and with the modified DJ¹ PESs. As before, our results computed with these two potentials are close to each other. However, one can see that our results and results from Refs.^{5,21} differ significantly. This happens particularly at low temperatures, for instance from 10 K to 50 K. Finally in this section, for the process $\text{HD}(2) + \text{H}_2(0) \rightarrow \text{HD}(0) + \text{H}_2(2)$ the difference between our $k_{j_1 j_2 \rightarrow j'_1 j'_2}(T)$ and the results from Ref.⁵ is about 3 orders of magnitude at $T=10$ K. The reason of this substantial deviation is not clear.

D. Application of the detailed balance principle

By using the time reversibility (reciprocity) principle one can obtain the detailed balance equation for the direct and reverse energy transfer processes or reactions⁴⁶. In the case of the inelastic scattering $a + b \rightleftharpoons a' + b'$

TABLE II. Results for three selected state-to-state rotational thermal rate coefficients $k_{j_1 j_2 \rightarrow j'_1 j'_2}(T)$ $\text{cm}^3 \text{s}^{-1}$ at various low temperatures T (K) in the $p\text{-H}_2(\alpha) + \text{HD}(\beta) \rightarrow p\text{-H}_2(\alpha') + \text{HD}(\beta')$ collisions. Calculations with different PESs: the original BMKP PES³¹ and the new modified DJ potential from this work. The corresponding older data from other authors^{5,21} are also included in this table. Numbers in parentheses are powers of 10.

T (K)	Rotational Thermal Rate Coefficients: $k_{j_1 j_2 \rightarrow j'_1 j'_2}(T)$ $\text{cm}^3 \text{s}^{-1}$											
	(02) \rightarrow (20)				(12) \rightarrow (20)				(20) \rightarrow (02)			
	BMKP	Mod. DJ	Ref. ²¹	Ref. ⁵	BMKP	Mod. DJ	Ref. ²¹	Ref. ⁵	BMKP	Mod. DJ	Ref. ²¹	Ref. ⁵
10	1.15(-11)	6.38(-12)		7.21(-15)	1.50(-13)	6.35(-14)		9.32(-14)	1.06(-17)	3.43(-18)		2.53(-20)
20	9.57(-12)	5.51(-12)		6.72(-15)	1.27(-13)	5.43(-14)		8.62(-14)	9.18(-14)	4.11(-15)		1.26(-17)
30	9.05(-12)	5.40(-12)		7.40(-15)	1.25(-13)	5.34(-14)		9.53(-14)	8.80(-14)	4.48(-14)		1.13(-16)
50	8.81(-12)	5.51(-12)	9.3(-13)	1.09(-14)	1.34(-13)	5.64(-14)	7.9(-14)	1.35(-13)	5.47(-13)	3.14(-13)	7.5(-14)	8.86(-16)
70	8.83(-12)	5.68(-12)		1.70(-14)	1.52(-13)	6.06(-14)		1.89(-13)	1.21(-12)	7.38(-13)		2.82(-15)
100	8.93(-12)	5.90(-12)	9.9(-13)	3.21(-14)	1.85(-13)	6.72(-14)	1.6(-13)	2.86(-13)	2.23(-12)	1.42(-12)	2.8(-13)	9.15(-15)
200	9.17(-12)	6.29(-12)	1.1(-12)	1.44(-13)	3.25(-13)	8.78(-14)	4.3(-13)	7.31(-13)	4.58(-12)	3.10(-12)	6.0(-13)	7.69(-14)
300	9.19(-12)	6.43(-12)		3.46(-13)	4.77(-13)	1.06(-13)		1.28(-12)	5.78(-12)	4.02(-12)		2.28(-13)

the detailed balance principle⁴⁶ relates the direct $a + b$ and the reverse $a' + b'$ processes and their cross sections $\sigma_{j_a j_b \rightarrow j'_a j'_b}^{ab}$ and $\sigma_{j'_a j'_b \rightarrow j_a j_b}^{a'b'}$:

$$(2j_a + 1)(2j_b + 1)p_{a \rightarrow b}^2 \sigma_{j_a j_b \rightarrow j'_a j'_b}^{ab}(E) = (2j'_a + 1)(2j'_b + 1)p_{b \rightarrow a}^2 \sigma_{j'_a j'_b \rightarrow j_a j_b}^{a'b'}(E). \quad (31)$$

Here, E is the total energy, $j_{a(b)}$ and $j'_{a(b)}$ are the initial and final rotational quantum numbers, $p_{a(a') \rightarrow b(b')}^2$ are the initial and final relative momenta between a and b species, $\sigma_{j_a j_b \rightarrow j'_a j'_b}^{ab}(E)$ and $\sigma_{j'_a j'_b \rightarrow j_a j_b}^{a'b'}(E)$ are direct and reverse integral cross sections respectively. The same type of the relationship can be obtained for the thermal rate coefficients $k_{j_1 j_2 \rightarrow j'_1 j'_2}(T)$. Let us rewrite Eq. (8) in the terms of the total energy E . Considering that the relative kinetic energy ϵ between a and b is Eq. (7), we compute the total energy from the lowest possible level between two channels. If it is associated with the second channel $a' + b'$, i.e. $j'_1 j'_2$ pair, the formula (8) becomes:

$$k_{j_1 j_2 \rightarrow j'_1 j'_2}^{ab}(T) = \frac{1}{(k_B T)^2} \sqrt{\frac{8k_B T}{\pi M_{12}}} \int_0^\infty \sigma_{j_1 j_2 \rightarrow j'_1 j'_2}(E) \times \frac{p_{ab}^2}{M_{12}} e^{-(E - \Delta E)/k_B T} dE. \quad (32)$$

Here, $\Delta E = [B_1 j_1(j_1 + 1) + B_2 j_2(j_2 + 1)] - [B_1 j'_1(j'_1 + 1) + B_2 j'_2(j'_2 + 1)]$ is the energy gap between the direct and reverse channels, and $\epsilon = p_{ab}^2/M_{12}$ is the kinetic energy. Now, for the reverse channel the thermal rate coefficient is:

$$k_{j'_1 j'_2 \rightarrow j_1 j_2}^{a'b'}(T) = \frac{1}{(k_B T)^2} \sqrt{\frac{8k_B T}{\pi M_{12}}} \int_0^\infty \sigma_{j'_1 j'_2 \rightarrow j_1 j_2}(E) \times \frac{p_{a'b'}^2}{M_{12}} e^{-E/k_B T} dE, \quad (33)$$

Comparing Eqs. (32) and (33) and taking into account Eq. (31) we obtain the detailed balance formula for the

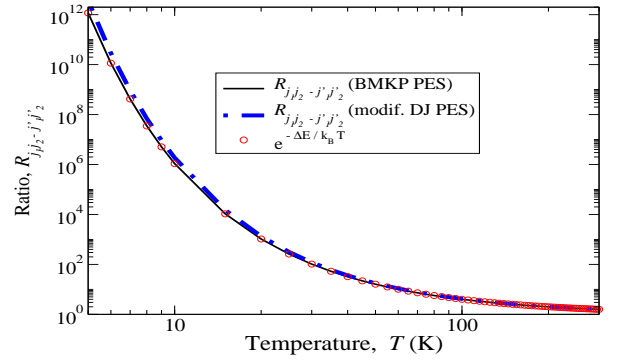
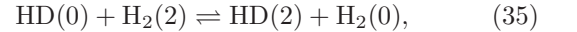


FIG. 9. (Color online) The ratio $R_{j_1 j_2 \rightleftharpoons j'_1 j'_2}(T)$ for the processes (35). Computation with the use of both potentials: the BMKP and the modified DJ PESs. The open circles are the values of the exponential function from the right side of Eq. (34).

thermal rate coefficients:

$$(2j_1 + 1)(2j_2 + 1)k_{j_1 j_2 \rightarrow j'_1 j'_2}^{ab}(T) = (2j'_1 + 1)(2j'_2 + 1) \times k_{j'_1 j'_2 \rightarrow j_1 j_2}^{a'b'}(T) e^{\Delta E/k_B T}. \quad (34)$$

The ratio $R_{j_1 j_2 \rightleftharpoons j'_1 j'_2}(T) = k_{j_1 j_2 \rightarrow j'_1 j'_2}^{ab}(T)/k_{j'_1 j'_2 \rightarrow j_1 j_2}^{a'b'}(T)$ is proportional to an exponent with the argument depending on ΔE . In this work we computed two direct-reverse processes in the HD + $p\text{-H}_2$ collisions, specifically:



with $\Delta E = 96.6 \text{ cm}^{-1}$. It would be useful to check how well the computed thermal rates (8) in this work satisfy the detailed balance equation (34). Fig. 9 represents these results. It is shown that all results are in a satisfactory agreement with each other.

IV. CONCLUSION

In this work a rotational method has been applied for the transformation of the 4-dimensional rigid monomer model $\text{H}_2\text{-H}_2$ PES of Ref.¹ to the non-symmetrical potential appropriate for calculations of the HD+H_2 collisions. Different low energy elastic and state-selected inelastic cross sections as well as the thermal rate coefficients for HD+H_2 have been computed and compared with previous calculations, where available. The rotational energy transfer in HD+H_2 is of importance for the thermodynamics of the ISM²⁴. By now few and rather conflicting results are available for the low energy HD+H_2 rotational energy transfer, see for example³⁸ and references therein. The BMKP PES³¹ has been already applied to HD+H_2 ^{37,38}. However, this PES may have failures. The fact was mentioned in Refs.^{12,13,34}. Therefore in this paper a new attempt has been undertaken to carry out alternative computational methods for HD+H_2 collision. In case of the BMKP and DJ PESs the necessary steps for each potential have been described in Secs. II B and II C and also in Ref.³⁷. In the case of the BMKP potential, which is a full six-dimensional surface³¹, the transformation from $\text{H}_2\text{-H}_2$ to the $\text{H}_2\text{-HD}$ system was done by shifting the center of mass in one H_2 molecule to the center of mass of the HD molecule. Because the DJ PES has been formulated for the rigid monomer rotor model, the transformation methodology was more complicated. Simply, the \vec{R}_1 and \vec{R}_2 coordinates are not available in this case, they have fixed lengths. In this paper the transformation has been accomplished by rotation of the space fixed $OXYZ$ coordinate system, i.e. by the redirection of the \vec{R}_3 vector. The new vector \vec{R}'_3 connects the center of masses of the H_2 and the HD molecules as shown in the Fig. 2. This procedure obtains new coordinate angles for the Jacobi vectors \vec{R}_1 , \vec{R}_2 , and \vec{R}_3 , and a new PES as in Eq. (20). New experiments that measure the state-to-state rotational cross sections in the $\text{HD}+o\text{-}p\text{-H}_2$ collisions at low temperatures are needed. Thereafter theoreticians and astrophysicists would be able to compare computational results with available experimental data. This type of work was recently accomplished, for instance, for the *para*- $\text{H}_2\text{+H}_2$ collision³³. Here it would be useful to mention other contributions on hydrogen-hydrogen collisions^{47–49}. Additionally, with the use of new HD+H_2 results for the thermal rate coefficients one could carry out new computation of the HD-cooling function mentioned in the introduction²⁴.

In conclusion, another interesting system worth mentioning is HD+HD . For this collision there are relatively old experimental state-to-state rotational probabilities for a few selected states⁵⁰. These old data can be useful in comparisons with the computational results obtained with different H_4 PESs: such as the available DJ and the BMKP PESs or some relatively new potentials, for example from work¹⁴. In the case of the DJ surface it would be possible to again apply the rotation procedure of the $OXYZ$ coordinate system as performed in this paper.

ACKNOWLEDGMENTS

This work was supported by Office of Sponsored Programs (OSP) and by Internal Grant Program of St. Cloud State University, and CNPq and FAPESP of Brazil.

- ¹P. Diep and J. K. Johnson, J. Chem. Phys. **112**, 4465 (2000); **113**, 3480 (2000).
- ²G. Zarur and H. Rabitz, J. Chem. Phys. **60**, 2057 (1974).
- ³S. Green, J. Chem. Phys. **62**, 2271 (1975).
- ⁴D.L. Johnson, R.S. Grace, and J.G. Skofronick, J. Chem. Phys. **71**, 4554 (1979).
- ⁵J. Schaefer, Astron. Astrophys. Suppl. Ser. **85**, 1101 (1990).
- ⁶D.R. Flower and E. Roueff, J. Phys. B: At. Mol. Opt. Phys. **32**, 3399 (1999).
- ⁷D.R. Flower, J. Phys. B: At. Mol. Opt. Phys. **33**, L193 (2000).
- ⁸D.R. Flower, J. Phys. B: At. Mol. Opt. Phys. **33**, 5243 (2000).
- ⁹S.K. Pogrebnya and D.C. Clary, Chem. Phys. Lett. **363**, 523 (2002).
- ¹⁰S.Y. Lin and H. Guo, Chem. Phys. **289**, 191 (2003).
- ¹¹F. Gatti, F. Otto, S. Sukiasyan, and H.-D. Meyer, J. Chem. Phys. **123**, 174311 (2005).
- ¹²R. A. Sultanov and D. Guster, Chem. Phys. **326**, 641 (2006).
- ¹³T.-G. Lee, N. Balakrishnan, R. C. Forrey, P. C. Stancil, D. R. Schultz, and G. J. Ferland, J. Chem. Phys. **125**, 114302 (2006); **126**, 179901 (2007).
- ¹⁴J. L. Belof, A. C. Stern, and B. Space, J. Chem. Theory Comput., **4** (8), 1332 (2008).
- ¹⁵G. Garberoglio and J.K. Johnson, ACS Nano, **4**, 1703 (2010).
- ¹⁶S.-I. Chu, J. Chem. Phys. **62**, 4089 (1975).
- ¹⁷U. Buck, Faraday Discuss. Chem. Soc. **73**, 187 (1982).
- ¹⁸D.W. Chandler and R.L. Farrow, J. Chem. Phys. **85**, 810 (1986).
- ¹⁹R.L. Farrow and D.W. Chandler, J. Chem. Phys. **89**, 1994 (1988).
- ²⁰D.R. Flower and E. Roueff, J. Phys. B: At. Mol. Opt. Phys. **31**, 2935 (1998).
- ²¹D. R. Flower, J. Phys. B **32**, 1755 (1999).
- ²²D. R. Flower and E. Roueff, J. Phys. B **32**, L171 (1999).
- ²³M. Born and R. Oppenheimer, Ann. Phys. **84**, 457 (1927).
- ²⁴A. Dalgarno and R. McCray, Ann. Rev. Astron. Astrophys. **10**, 375 (1972).
- ²⁵V. Roudnev and M. Cavagnero, Phys. Rev. A **79**, 014701 (2009).
- ²⁶R. C. Forrey, Phys. Rev. A **66**, 023411 (2002).
- ²⁷A. V. Avdeenkov and J. L. Bohn, Phys. Rev. A **71**, 022706 (2005).
- ²⁸D. S. Petrov, C. Salomon and G. V. Shlyapnikov, Phys. Rev. A **71**, 012708 (2005).
- ²⁹A. V. Avdeenkov and J. L. Bohn, Phys. Rev. A **64**, 052703 (2001); **66**, 052718 (2002).
- ³⁰D. W. Schwenke, J. Chem. Phys. **89**, 2076 (1988).
- ³¹A. I. Boothroyd, P. G. Martin, W. J. Keogh, and M. J. Peterson, J. Chem. Phys. **116**, 666 (2002).
- ³²S.Y. Lin and H. Guo, J. Chem. Phys. **117**, 5183 (2002).
- ³³B. Mat, F. Thibault, G. Tejeda, J. M. Fernandez, and S. Montero, J. Chem. Phys. **122**, 064313 (2005).
- ³⁴R. A. Sultanov and D. Guster, Chem. Phys. Lett. **428**, 227 (2006).
- ³⁵F. Otto, F. Gatti, and H.D. Meyer, J. Chem. Phys. **128**, 064305 (2008).
- ³⁶F. Otto, F. Gatti, and H.D. Meyer, J. Chem. Phys. **131**, 049901 (2009).
- ³⁷R. A. Sultanov and D. Guster, Chem. Phys. Lett. **436**, 19 (2007).
- ³⁸R. A. Sultanov, A. V. Khugaev, and D. Guster, Chem. Phys. Lett. **475**, 175 (2009).
- ³⁹S. Green, J. Chem. Phys. **67**, 715 (1977).
- ⁴⁰*Modern Theoretical Chemistry: Dynamics of Molecular Collisions*, Eds. W. H. Miller (Plenum, New York, 1976).
- ⁴¹J. M. Hutson and S. Green, *MOLSCAT Computer Code version 14*, (Distributed by Collaborative Comp. Proj. 6 of the Engi-

- neering and Physical Sciences Research Council, Daresbury Lab., 1994).
- ⁴²R.A. Sultanov, D. Guster, and S.K. Adhikari, *Proc. of The 2010 NASA Lab. Astrophys. Workshop*, Gatlinburg, Tennessee, Oct. 25-28, 2010, Ed. D.R. Schultz (ORNL), C-22 (4 pages).
- ⁴³L. Machin and E. Roueff, *Astron. & Astrophys.* **460**, 953 (2006); **465**, 647 (2007).
- ⁴⁴D. A. Varshalovich, A. N. Moskalev, and V. K. Khersonskii, *Quantum Theory of Angular Momentum*, (World Scientific, Singapore, 1988); H. Goldstein, *Classical Mechanics*, (Addison-Wesley Publ. Co. Inc., London, England, 1959).
- ⁴⁵E. W. Weisstein, *Euler's Rotation Theorem*, from MathWorld: A Wolfram Web Resource (Wolfram Mathematica): <http://mathworld.wolfram.com/EulersRotationTheorem.html>.
- ⁴⁶L. D. Landau and E. M. Lifshitz, *Quantum Mechanics, Non-Relativistic Theory*, Third Edition, Course of Theoretical Physics, Volume 3, (Butterworth-Heinemann, 2003).
- ⁴⁷T. Kusakabe, L. Pichl, R. J. Buenker, M. Kimura, and H. Tawara, *Phys. Rev. A* **70**, 052710 (2004).
- ⁴⁸W. Meyer, L. Frommhold, and G. Birnbaum, *Phys. Rev. A* **39**, 2434 (1989).
- ⁴⁹S. P. Reddy, G. Varghese, and R. D. G. Prasad, *Phys. Rev. A* **15**, 975 (1977).
- ⁵⁰W. R. Gentry and C. F. Giese, *Phys. Rev. Lett.* **39**, 1259 (1977).

(Dated: February 16, 2019)

Abstract

